DOI: 10.1002/chem.200500613

Micelles for the Self-Assembly of "Off–On–Off" Fluorescent Sensors for pH Windows

Yuri Diaz-Fernandez,[b] Francesco Foti,[a] Carlo Mangano,[a] Piersandro Pallavicini,*[a] Stefano Patroni,[a] Aurora Perez-Gramatges,[b] and Simon Rodriguez-Calvo[b]

Abstract: A micellar approach is proposed to build a series of systems featuring an "off–on–off" fluorescent window response with changes in pH. The solubilizing properties of micelles are used to self-assemble, in water, plain pyrene with lipophilized pyridine and tertiary amine moieties. Since these components are contained in the small volume of the same micelle, pyrene fluorescence is influenced by the basic moieties: protonated pyridines and free tertiary amines behave as quenchers. Accordingly, fluorescence transitions from the "off" to the "on" state, and viceversa, take place when the pH crosses the pK_a values of the amine and pyridine fragments. To obtain an "off–on–off" fluorescent response in this investigation we use either a set of dibasic lipophilic molecules (containing covalently linked pyridine and tertiary amine groups) or combinations of separate, lipophilic pyridines and tertiary amines. The use of combinations of dibasic and monobasic lipophilic molecules also gives a window-shaped fluorescence response with changes in pH: it is the highest pyridine pK_a and the lowest tertiary amine pK_a that determine the window limits. The pK_a values of all the examined lipophilic molecules were determined in micelles, and compared with the values found for the same molecules in solvent mixtures in which they are molecularly dispersed. The effect of micellization is to significantly lower the observed protonation constants of the lipophilized species. Moreover, the more lipophilic a molecule is, the lower the observed log$K$ value is. Accordingly, changing the substituents on the basic moieties or modifying their structure, tuning the lipophilicity of the mono- or dibases, and choosing among a large set of possible combination of lipophilized mono- and dibases have allowed us to tune, almost at will, both the width and the position along the pH axis of the obtained fluorescent window.

Keywords: fluorescence · micelles · molecular devices · sensors

Introduction

The possibility offered by working in water and confining separate hydrophobic fluorophores and quenchers in the small volume of the same micelle has been exploited in surfactant science since the early 1970s. The observation of either steady-state or dynamic fluorescence quenching due to intramicellar interactions between for example, pyrene and a series of quenchers (typically *N*,*N*′-dibutyl aniline[1] and dodecylpyridinium[2]) is a well-established method to calculate the aggregation number (AN), that is, the average number of surfactant units per single micelle. Kinetics parameters, such as the rate constants of the processes involving the fluorophore/quencher systems inside a micelle, have also been elucidated by means of fluorescence quenching[3]. Sophisticated structural parameters, such as the position of a hydrophobic molecule inside a micelle with respect to the water/micelle interface[4] or the shape of a micelle,[5] have also been investigated through intramicellar quenching processes between separated components. Another branch of chemistry, fluorescent sensing of cations, anions and neutral species, has developed dramatically[6] after the first examples

[a] Dr. F. Foti, Dr. C. Mangano, Dr. P. Pallavicini, Dr. S. Patroni
Dipartimento di Chimica Generale
Università di Pavia, via Taramelli
12-27100 Pavia (Italy)
Fax: (+39) 038-252-8544
E-mail: psp@unipv.it

[b] Dr. Y. Diaz-Fernandez, Prof. A. Perez-Gramatges, Prof. S. Rodriguez-Calvo
Instituto Superior de Tecnologias y Ciencias Aplicada
Department of Radiochemistry, Ave Salvador Allende y Luaces
Plaza de la Revoluciòn, Ciudad de la Habana
Apartado Postal 16040, Habana 11600 (Cuba)

Supporting information for this article is available on the WWW under http://www.chemeurj.org/ or from the author.

published as early as 1988.[7] These examples were based on a traditional molecular approach, in which a fluorophore and a receptor component, also capable of acting as quencher in the absence ("off–on" sensor) or in the presence ("on–off" sensor) of the target species, were covalently linked by a spacer. Stressing that this approach often requires tedious synthetic efforts, it is surprising that only the new millennium brought the idea of using micelles as containers for preparing supramolecular sensors in which simple, separated fluorophores and receptors/quenchers are kept together and communicate inside the micelle without the need of building a covalent structure. Tecilla, Tonellato et al. have shown how Cu^{2+} can be signalled for by fluorescence quenching when it is coordinated by a lipophilized dipeptide inside CTAB (cetyltrimethylammonium bromide) micelles. These micelles also contained the lipophilic 8-anilino-1-naphthalenesulfonic acid fluorophore,[8] or, in a similar system, the Rhodamine 6G fluorophore.[9] Anslyn and Niikura demonstrated that the neutral surfactant Triton X-100 allows the detection of the IP (inositol triphosphate) anion in water, thanks to enhanced ion-pair-driven molecular recognition between a hydrophobic anion receptor, IP, and the competing anionic lipophilic fluorophore 5-carboxyfluorescein inside the micelles.[10] Recently, we published a contribution describing a sensing system selective for Ni^{2+} and Cu^{2+} based on a lipophilized diamino–diamido ligand and pyrene, which interacted inside Triton X-100 micelles.[11]

Since we are also interested in the study of fluorescent sensors for pH, and, in particular, of those capable of giving a window-shaped I_f versus pH response (I_f = fluorescence intensity),[12] we decided to also apply the supramolecular micellar approach to these kinds of systems. Window-shaped sensors for pH may be important for life sciences, as biological processes are known to be effective only in restricted concentration ranges of the involved species and, in particular, in restricted pH ranges. However, designing and building systems of this kind is a complicated matter and only few papers have been published reporting an "off–on–off" or "on–off–on" I_f versus pH window. Moreover, beside a very recent example based on an Eu^{III}-luminescent complex of a tetraquinoline-substituted cyclen ligand,[13] and another example published by our group based on multicomponent coordination complexes,[12b,c] all the described systems are organic molecules that have to be built by step-by-step organic synthesis.[14] These molecular systems are based on the original approach of de Silva and co-workers.[14a] Here anthracene was the light-emitting component and was covalently linked to one or more pyridine and tertiary amino groups, that behaved as pH-dependent quenching fragments, through spacer units. Three states are available in these kind of molecules as a function of pH (described in Scheme 1): i) at low pH both pyridine and amine are protonated (form **A**) and the fluorescence is "off", with the pyridineH^+ fragment acting as a quencher by photoelectron transfer (PET) thanks to its electron-acceptor properties; ii) as the pH rises above the pyridine pK_a, this fragment is no longer protonated (while the amine still is: form **B**) and thus the fluorescence goes "on"; iii) as the pH is increased further above the amine pK_a, this group also becomes nonprotonated, the molecule is neutral (form **C**) and the fluorescence turns "off" again due to the quenching properties (by PET) of the electron-donating tertiary amino groups.

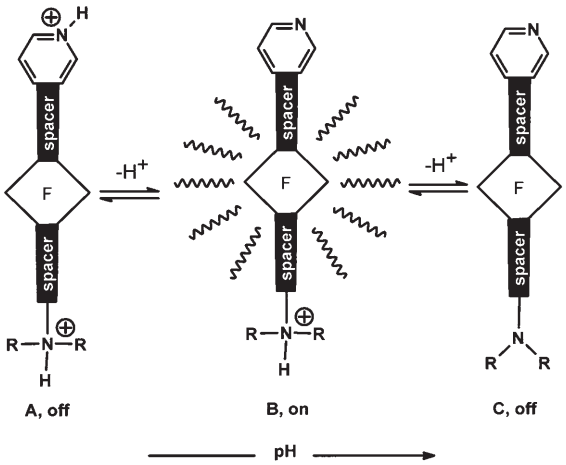

Scheme 1. Working scheme for the covalent approach to window-shaped fluorescent sensors for pH. Component **F** is a fluorophore (typically anthracene, see refs. [13a–d], the "spacer" may be as simple as a CH_2 unit. Transition from A to B takes place when pH crosses the pyridinium pK_a value; transition from B to C takes place when pH crosses the ammonium pK_a value.

The approach to "off–on–off" fluorescent sensors for pH windows that we describe in this paper merges the ideas presented by de Silva and co-workers with the flexibility of the micelle-as-container approach: lipophilized pyridines and amines are used as pH-dependent quenchers and pyrene is the fluorophore. However, since these components are not (or only partially) covalently linked, but rather self-assembled inside a micelle, synthetic efforts are reduced to the minimum.

Results and Discussion

Protonation constants in the water/micelle medium: We have investigated a set of lipophilized molecules, each one containing either one pyridine or one trialkylamine group, or both. *N*,*N*′-Dimethyl-*N*″-dodecylamine (**DAm**) is commercially available, while the remaining six molecules were obtained through simple syntheses (see Experimental Section). They are all insoluble in water, at least in their neutral form. They readily dissolve in water containing the neutral surfactant TritonX-100 above its critical micelle concentration (cmc), thanks to the insertion of their lipophilic tails in the micellar core. Triton X-100 is a classical surfactant that is widely employed and whose properties are well-established.[15] Moreover, since it is neutral, no electrostatic effects are to be expected for protonation/deprotonation properties of any species included inside its micelles. Unless otherwise stated, in the experiments run for this investigation we have operated with a surfactant concentration of 6.47 g L^{-1}. Triton

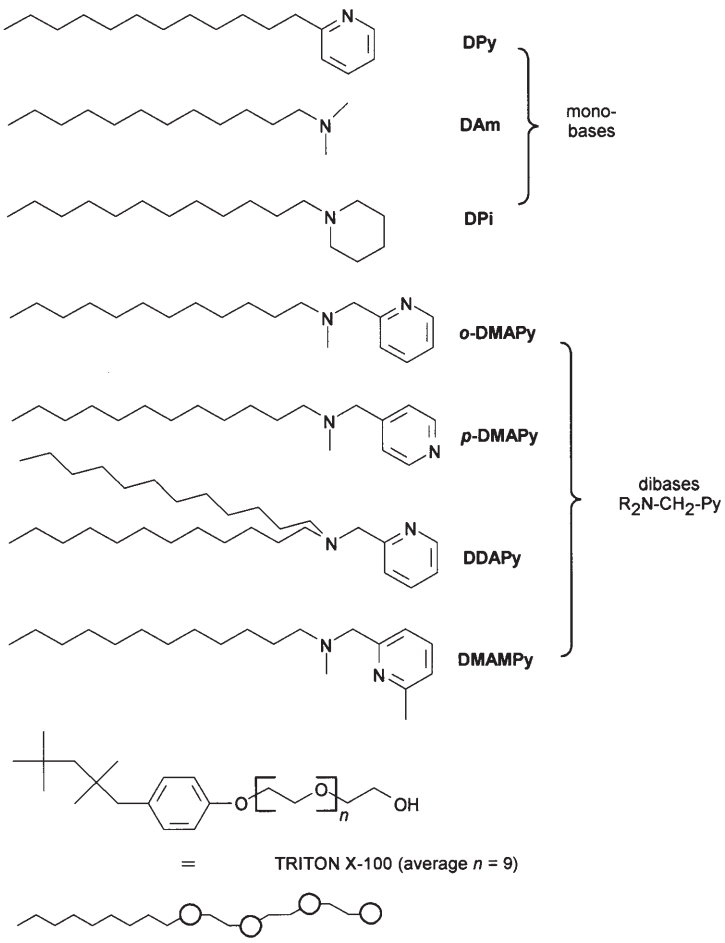

X-100 has a cmc of $\sim 2\times10^{-4}$ M and an aggregation number of 111.[15b] Since the average molecular weight of the commercial Triton X-100 that we used was 647, we were operating with an average micelle concentration of $\sim 10^{-4}$ M. We used concentrations of lipophilized bases equal or lower than 10^{-3} M, so that a maximum average of 10 base molecules per micelle is to be expected. This was done in order to minimize base–base interactions and to avoid significant changes in the micelle parameters with respect to pure surfactant (we have already shown that, for example, the AN does not change significantly for inclusion of up to 10 molecules equipped with a C_{12} tail and possessing analogous acid/base properties to those presented in this paper[5]).

As a first step, we examined the acid/base properties in the water–surfactant medium for each lipophilized base, using a standard potentiometric titration apparatus and well-established experimental procedures (see Experimental Section), that is, measuring a space-averaged value of E with a macroscopic glass electrode in an excess acid solution to which standard base was added in 10–20 μL portions. From the titration data we calculated the protonation constants of the examined bases, corresponding to the pK_a of their protonated species.[16] These values are of course not "intrinsic" but "observed", that is, influenced by the fact that the lipophilic bases are included inside micelles, with the organic tail inserted in the hydrophobic micellar core and the more polar head presumably lying in the hydrophilic, external layer of the micelle. Penetration of the solvent and any dissolved species into the hydrophilic layer of the micelle is partially allowed, but the local concentration of water and H^+ could be significantly lower with respect to the bulk solution.[4] Hence, taking into account both lower local $[H^+]$ and a less efficient solvation of protonated species, we expected lower observed protonation constant values with respect to the appropriate references, that is, nonlipophilic bases triethylamine and 2-methylpyridine in water. Moreover, it has already been shown how the lowering of the measured protonation constants is proportional to the lipophilicity of the considered base,[4] that is, to the depth of its inclusion in the micelle, as this is inversely proportional to the efficiency of solvation of the protonated species. The found values are reported in Tables 1 and 2,

Table 1. Logarithmic protonation constants for the monobasic molecules. Uncertainties are reported in parentheses. The K values refer to the formation equilibria, base $+ H^+ = [baseH]^+$.

	log$K$
Dpy	3.73(0.02)
DAm	7.84(0.01)
DPi	7.38(0.02)

Table 2. Step logarithmic protonation constants for the dibasic molecules. Uncertainties are reported in parentheses. The K values refer to protonation equilibria. In particular, K_1 refers to Equilibrium (1), see text, and it is relative to the protonation of the amino moiety. K_2 refers to Equilibrium (2), see text, and it is relative to the protonation of the pyridine moiety.

	logK_1	logK_2
o-DMAPy	6.27(0.01)	2.13(0.03)
p-DMAPy	5.41(0.01)	2.23(0.03)
DDAPy	4.58(0.01)	1.8 (0.1)
DMAMPy	6.31(0.02)	2.06(0.04)

and confirm the expected trend. The log$K$ values for protonation of the reference compounds triethylamine and 2-methylpyridine in water are 10.68[17] and 6.06, respectively.[18] Moreover, an even better molecule for comparison with the cyclic monobase *N*-dodecylpiperidine, **DPi**, is *N*-methylpiperidine, with a log$K$ value of 10.13.[17] The values found for the monobases 2-dodecylpyridine (**DPy**), **DAm** and **DPi** show that lipophilization and inclusion in micelles significantly lower the log$K$ value by ~2–3 log units with respect to the water-soluble reference bases. This micellization effect is also confirmed by the determination of the protonation constants for the monobases **DPy**, **DAm** and **DPi** in the organic-enriched solvent mixture dioxane/water (8:2 v/v). In this mixture the three molecules cannot form micelles and are molecularly dispersed. We found log$K = 4.14(\pm0.02)$ for **DPy**, log$K = 8.55(\pm0.01)$ for **DAm** and log$K = 8.48$ (±0.04) for **DPi**. These values are still lower then those found in water for 2-methylpyridine, triethylamine and *N*-methylpi-

peridine; the difference is due to the intrinsic lower solvation ability of any organic-enriched aqueous solvent with respect to water. However, we also measured the protonation constants for 2-methylpyridine, triethylamine, and *N*-methylpiperidine in dioxane/water (8:2 v/v). We found the log*K* values very similar to those of **DPy**, **DAm** and **DPi** in the same medium, that is, 4.41(±0.01), 9.20(±0.01) and 8.66 (±0.03), respectively. Consequently, the huge differences found between the log*K* values for water-dispersed and water-micellized analogous base moieties can be assigned to their inclusion in micelles.

When the protonation constants of the dibasic molecules, which can be schematized as $R_2N\text{-}CH_2\text{-}Py$, are considered (Table 2), the proximity of the pyridine and amine moieties, which are separated only by a $\text{-}CH_2\text{-}$ unit, is the origin of even lower values. In Table 2 the logK_1 values for the dibases pertain to the more basic amino group, that is, refer to Equilibrium (1).

$$R_2N\text{-}CH_2\text{-}Py + H^+ \rightleftharpoons [R_2NH\text{-}CH_2\text{-}Py]^+ \quad (1)$$

and vary between 4.58 (**DDAPy**) and 6.31 (**DMAMpy**). The further lowering of the log*K* values of the tertiary amine moieties with respect to **DAm** and **DPi** is due to the increased steric hindrance and lipophilicity introduced by the pyridine group (which is nonprotonated at the pH values at which Equilibrium (1) takes place). It is noteworthy that the didodecylated molecule **DDAPy** has a logK_1 value as low as 4.58. This low value is due to its increased hydrophobicity because of the location of the amino group closer to the micellar core and far away from the water–micelle interface.[4] On the other hand, all the logK_2 values, corresponding to the protonation of the pyridine group [Equilibrium (2)].

$$[R_2NH\text{-}CH_2\text{-}Py]^+ + H^+ \rightleftharpoons [R_2NH\text{-}CH_2\text{-}PyH]^{2+} \quad (2)$$

are dramatically low in the micelle/water medium. This is due to the electrostatic repulsion exerted by the proximate ammonium group (the tertiary amines are already protonated at the pH values where the pyridines become protonated), that adds to the micellization effect. Noticeably, lowering of logK_2 is also observed for the *para*-derivative ***p*-DMAPy**, suggesting that not only an electrostatic through-space effect, but also a through-bond inductive effect is playing a significant role. The roles of both micellization and the ammonium proximity were confirmed by determining the protonation constants of the representative ***o*-DMAPy** molecule in dioxane/water (8:2 v/v). In this case we found logK_1 = 7.08 (±0.05) and logK_2 = 2.59 (±0.05). Interestingly, it can be noted that the Δlog*K* values, that is, the difference between the log*K* found in dioxane/water and in water/micelle media are 0.41 for **DPy** and 0.71 for **Dam**. These values match well with the Δlog*K* of 0.46 and 0.81 found in ***o*-DMAPy** for the protonation of its pyridine and amine moieties, suggesting an analogous contribution of the micellization effect in both cases.

Finally, from the log*K* values listed in Tables 1 and 2, the distribution diagrams, that is, % of species (relative to total lipophilic base) versus pH, can be drawn.[19] These diagrams will be used in the following sections to relate the found I_f versus pH profiles to the species in equilibrium in the examined pH ranges.

"On–Off" fluorescent pH sensors from the monobasic molecules: Prior to any experiment involving lipophilic bases, the fluorescence of pyrene was checked at a concentration of 9×10^{-6} M (the value was kept constant for all the experiments described), in water containing Triton X-100 at the usual concentration. Under these conditions, an average of ~0.1 pyrene molecules per micelle can be calculated. The value is kept so low both because of the intense pyrene fluorescence and to avoid any possible formation of pyrene–pyrene excimers (which derives from the inclusion in the same micelle of two or more pyrene units). Coupled pH–spectrofluorimetric titrations in the 0–12 pH range confirmed that the emission of pyrene is constant.[20] We then also examined pyrene fluorescence in the same pH range in the presence of either triethylamine or 2-methylpyridine (10^{-3} M in each case). Both these species are water soluble and are not expected to interact significantly with the micelles. Accordingly, also in this case, no variations in the pyrene fluorescence was observed in the 0–12 pH range.

Coupled pH–spectrofluorimetric titrations were then performed to determine the variation of the fluorescence of pyrene with pH within the same range for solutions containing one of the monobases (**DPy**, **DMa**, or **DPi**) at a concentration of 10^{-3} M. An average of 10 molecules of base is expected for each micelle at this concentration, so that any micellized pyrene should experience this average number of pH-sensitive quenchers in its micelle. As expected, in all cases a sigmoidal fluorescence intensity trend was found with a change in pH; that, on going from low to high pH, is of the "off–on" type for the 2-dodecylpyridine derivative and of the "on–off" type for the two dodecylated tertiary amines. In particular, fluorescence goes "on" or "off" when the pH is increased above the bases' pK_a values. Figure 1a reports the series of spectra obtained at various pH values in the representative case of **DPy** (analogous emission spectra have been obtained for all the other fluorescence versus pH measurements in this work). A better visualization is obtained by plotting I_f at 392 nm, that is, at the wavelength of pyrene maximum emission, as a function of pH. Figure 1b–d displays $I_{f,392}$ versus pH profiles for the three monobases, superimposed to the relative distribution diagrams.

A close superposition of the I_f versus pH profiles is observed with the distribution diagrams, as shown in Figure 1b–d. In particular, Figure 1b shows that the fluorescence goes "on" (black triangles) when the $[\mathbf{DPy}H]^+$ deprotonates to form free **DPy**, while Figure 1c and d show that the fluorescence goes "off" when the tertiary amino group of $[\mathbf{DMa}H]^+$ and $[\mathbf{DPi}H]^+$ deprotonates to form free **DMa** and **DPi**. Although we do not have any experimental information on the nature of the quenching process, the ob-

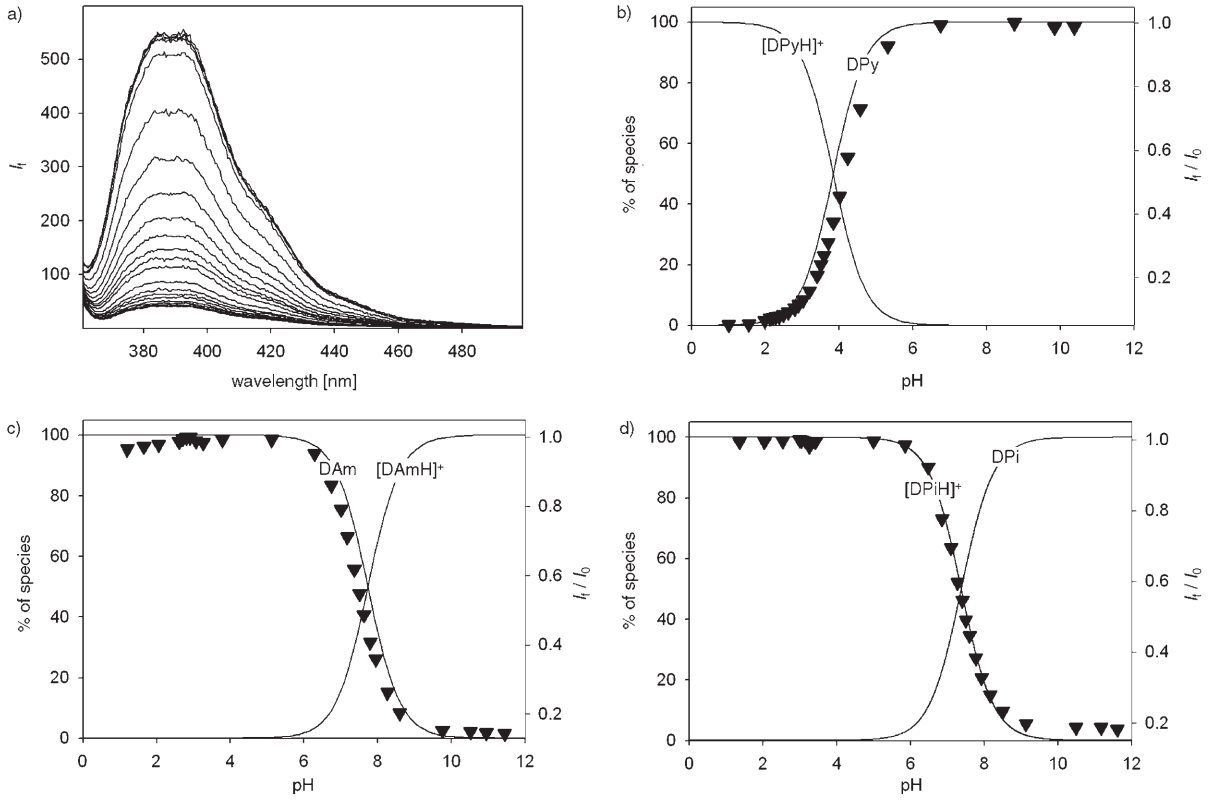

Figure 1. a) Series of pyrene emission spectra obtained for the system containing the DPy monobase at various pH. Superimposable, low-intensity spectra are obtained at low pH values (<2), intensity starts to increase at pH>2.5, and superimposable full-emission spectra are obtained at pH > 6.5. b–d) Black triangles represent the relative emission intensity (I_f/I_0) at 392 nm with varying pH (the maximum found emission in each series of spectra is considered as I_0). Solid lines represent the % (with respect to total base) of each species present at the equilibrium with varying pH. The species pertaining to each profile are indicated on the plots.

vious hypothesis that intramicellar photo-electron transfer mechanisms are still valid can be proposed; protonated pyridines are good electron acceptors and free tertiary amines good electron donors and both are well-known PET quenchers from/to the excited state of polyaromatic molecules.[14]

An "off–on–off" fluorescent pH sensor from the dibasic molecules: In the case of the dibasic molecules ***o*-DMAPy**, ***p*-DMAPy**, **DDAPy** and **DMAMPy**, the I_f versus pH behaviour has also been examined by means of pH–fluorimetric titrations for each molecule in the 0–12 pH range. The solutions contained 10^{-3} M bases, that is, with an average of 10 base molecules per micelle. In this situation, any micelle containing pyrene is a supramolecular system resembling the "classical" covalently linked molecular systems for fluorescent signalling of pH windows[14] described in Scheme 1: although the molecules are not directly connected, pyrene experiences the presence of pyridine and tertiary amino groups in the small micellar volume. Accordingly, an "off–on–off" I_f versus pH profile is to be expected on going from low to high pH values or viceversa, as it is pictorially shown in Scheme 2.

This behaviour is indeed what is found for the four systems, with the window limits determined by the log$K$ values of the pyridine and amine moieties, that is, by the pK_a of their protonated forms. As it can be seen in Figure 2a–d, a fair superposition is observed between $I_{f,392}$ versus pH profiles (black triangles) and species distribution (solid lines). In particular, fluorescence is "off" when the base molecules are in the diprotonated $[R_2NH\text{-}CH_2\text{-}PyH]^{2+}$ form, with micelles containing a pyridinium fragment; fluorescence goes "on" when the pH is raised above the pK_a value of pyridinium, so that the pyridine fragment deprotonates and the monoprotonated species $[R_2NH\text{-}CH_2\text{-}Py]^+$ is obtained. Finally, fluorescence is "off" again when the pH is sufficiently high to be above the ammonium pK_a value, so that the tertiary amine group is deprotonated to give the neutral $R_2N\text{-}CH_2\text{-}Py$ species.

Quite interestingly, the data shown in Figure 2 merged with those in Table 1 illustrate the versatility of this approach. The window limits are regulated by the log$K$ values of the micellized molecules and thus can be tuned by playing with substituents or with the lipophilicity of the whole molecule. Figure 3 shows the amplitude and the limits of the fluorescent pH windows described by the systems presented in this paper. The horizontal segments connect, for each system, the pH values corresponding to the pK_a of the species responsible for the quenching process. However, switching of I_f from the "off" to the "on" state, or viceversa, is not, of course, a vertical transition with respect to the pH

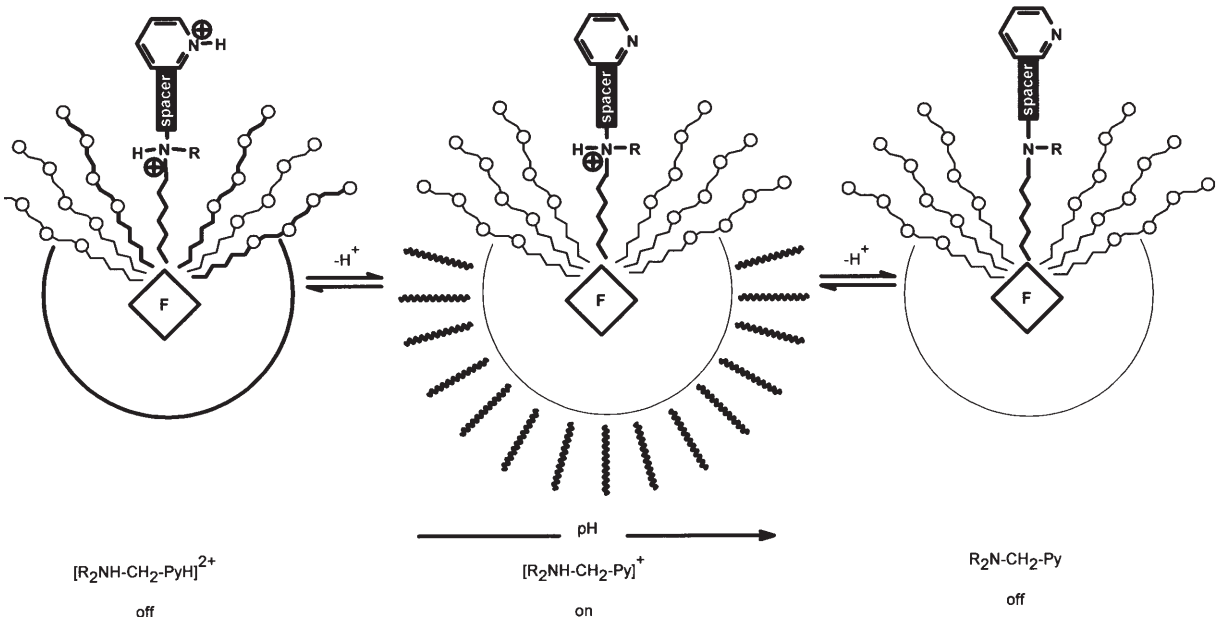

Scheme 2. Working scheme for the micelle-contained systems based on lipophilic dibases (**F** = pyrene). The "spacer" component is always CH_2, connected to the pyridine ring in an *ortho*- or *para*-position. Transitions from one form to the other take place with the pH increased above the pK_a of the involved base.

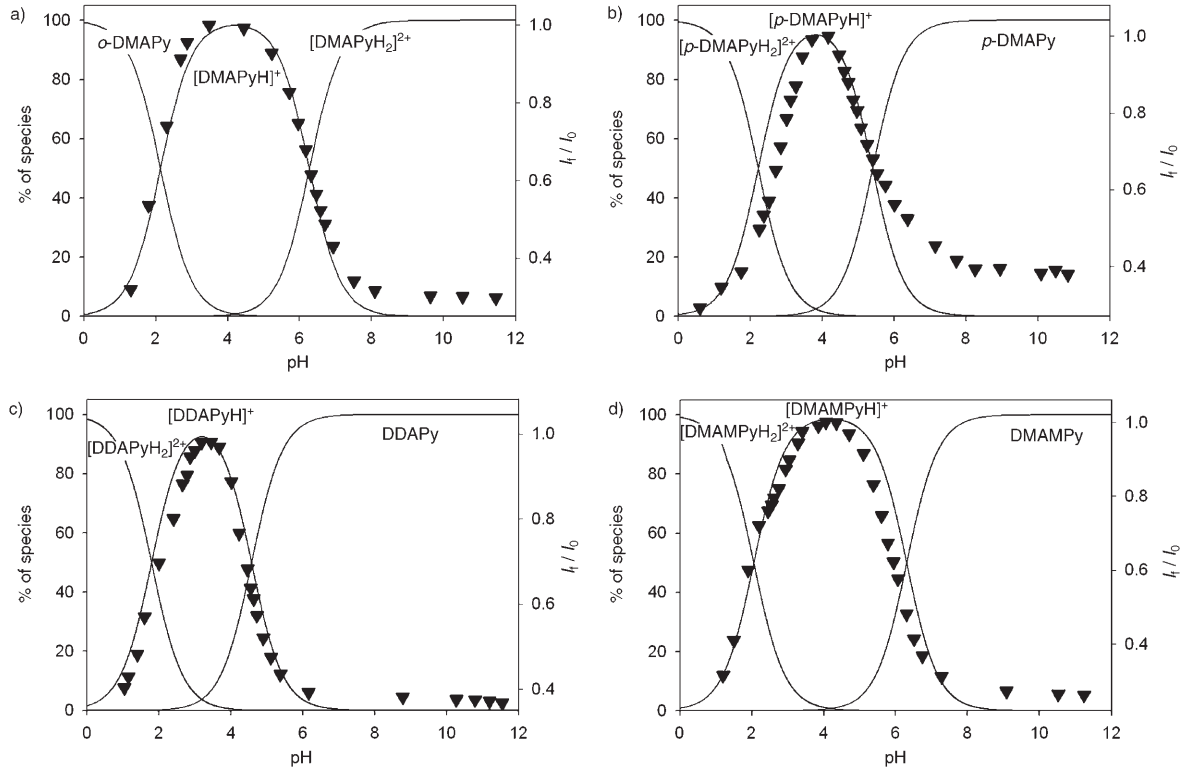

Figure 2. Black triangles represent the relative emission intensity (I_f/I_0) at 392 nm with varying pH (the maximum found emission in each series of spectra is considered as I_0). Solid lines represent the % (with respect to total base) of each species present at the equilibrium with varying pH. The species pertaining to each profile are indicated on the plots.

axis. This transition follows a smooth curve along the distribution diagram of the pertinent species, so that the resulting I_f versus pH profile follows a curve resembling a bell-shaped one. Accordingly, the horizontal segments of Figure 3 more appropriately represents the half-height width of the bell-shaped I_f versus pH curves.

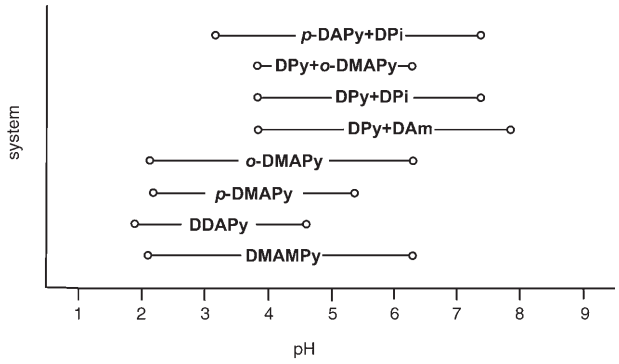

Figure 3. Horizontal segments represent the ideal half-height width of the I_f versus pH curves of each system. Their limiting values on the pH scale correspond to the pK_a values of base moieties responsible of the quenching processes.

"Off–On–Off" fluorescent pH sensor from the combination of two basic molecules: The flexibility of the micellar approach can be further exploited by using combinations of monobases, or even combinations of monobases and dibases with pyrene to build, in the same micelle, a system similar to the covalent ones described in Scheme 1. In the simplest case, all that is needed is to introduce one lipophilized pyridine and one lipophilized tertiary amine in the same micelle in the presence of pyrene. As it is pictorially described by Scheme 3, what is obtained is an "off–on–off" signalling system delimited by the pK_a values of the pyridine and tertiary amine moieties.

A combination of the two monobases **DAm** and **Dpy** was obtained by operating in a pyrene/Triton X-100 solution containing both bases in 5×10^{-4} M concentration, that is, with an average of five molecules of each base per micelle. Any reciprocal influence of the two molecules on their acid–base properties can be excluded: we again performed a potentiometric titration on solutions containing Triton X-100 and the two bases at 5×10^{-4} M concentration and obtained the same log$K$ values found with the titrations carried out with just one micellized species at a concentration of 10^{-3} M. By means of pH–fluorimetric titrations, a very satisfactory "off–on–off" I_f versus pH profile was found (see Figure 4a, black triangles), which clearly comes from the merging of the I_f versus pH profiles displayed in Figure 1a and b. In Figure 4a the fluorescence intensity profile is superimposed on a distribution diagram calculated for the system containing both **DPy** and **DAm** in 5×10^{-4} M concentration. It can be seen that the fluorescence is switched "off" at low pH values where the quencher [**DPy**H]$^+$ coexists with [**DAm**H]$^+$, is switched "on" where **DPy**/[**DAm**H]$^+$ coexist, and is switched "off" again where the quencher **DAm** coexists with **DPy**. When the same kind of experiment is repeated with the **DPy**/**DPi** system, we obtained the same type of profile (Figure 4b, black triangles), but with the upper pH limit of the window shifted by ~0.5 units to the left due to the analogous difference in the log$K$ values between **DAm** and **DPi** (see Table 1).

Noticeably, two different amines or two different pyridines can coexist in the same micelle, with the "off" limits being dictated by the higher pyridine pK_a and lower amine pK_a. This suggests the possibility to also vary the combination of monobases and dibases to shift the window position along the pH axis, or to obtain larger or narrower windows. Accordingly, we have combined a monobase, **DPy**, with a dibase, ***o*-DMAPy** (both at 5×10^{-4} M concentration). In this case, the tertiary amine of ***o*-DMAPy** sets the upper window limit with its log$K$ value of 6.27. It is therefore the more basic of the two coexisting pyridines (i.e., that belonging to **DPy**) that regulates the lower window limit with its log$K$ value of 3.73, thus allowing to obtain another fluorescent

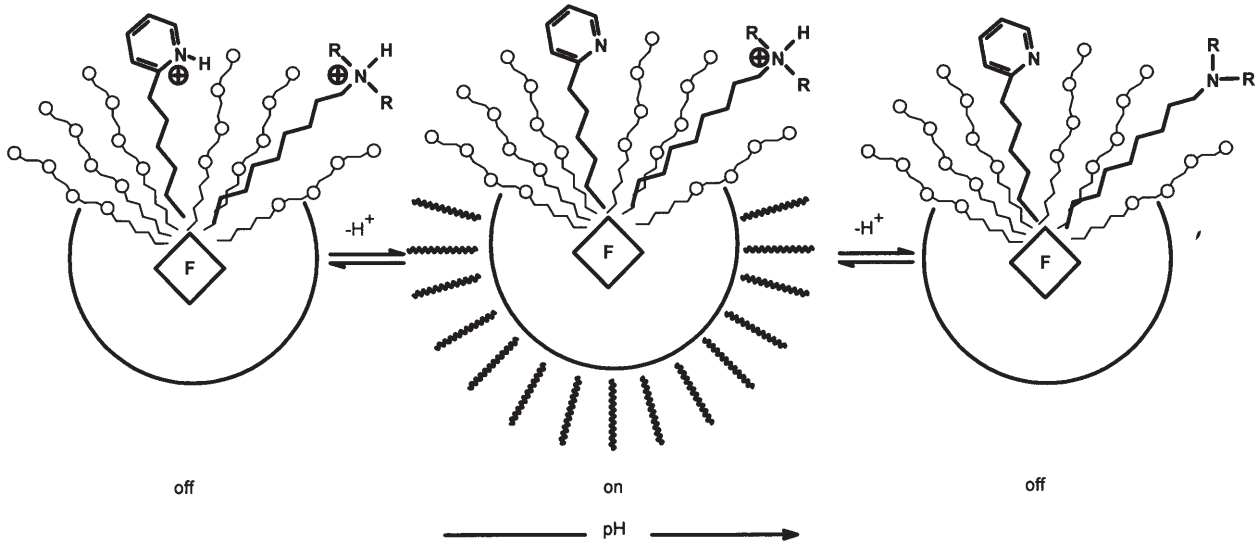

Scheme 3. Working scheme for the system based on the combination of one pyridine and one tertiary amine monobases (**F** = pyrene, the pyridine-containing component is **DPy**, the tertiary-amine-containing component may be **DAm** or **DPi**). Low pH passage from the "off" to the "on" form takes place at pH values crossing **DPy** pK_a. High pH passage from the "on" to the "off" form takes place at pH values crossing **DAm** or **DPi** pK_a.

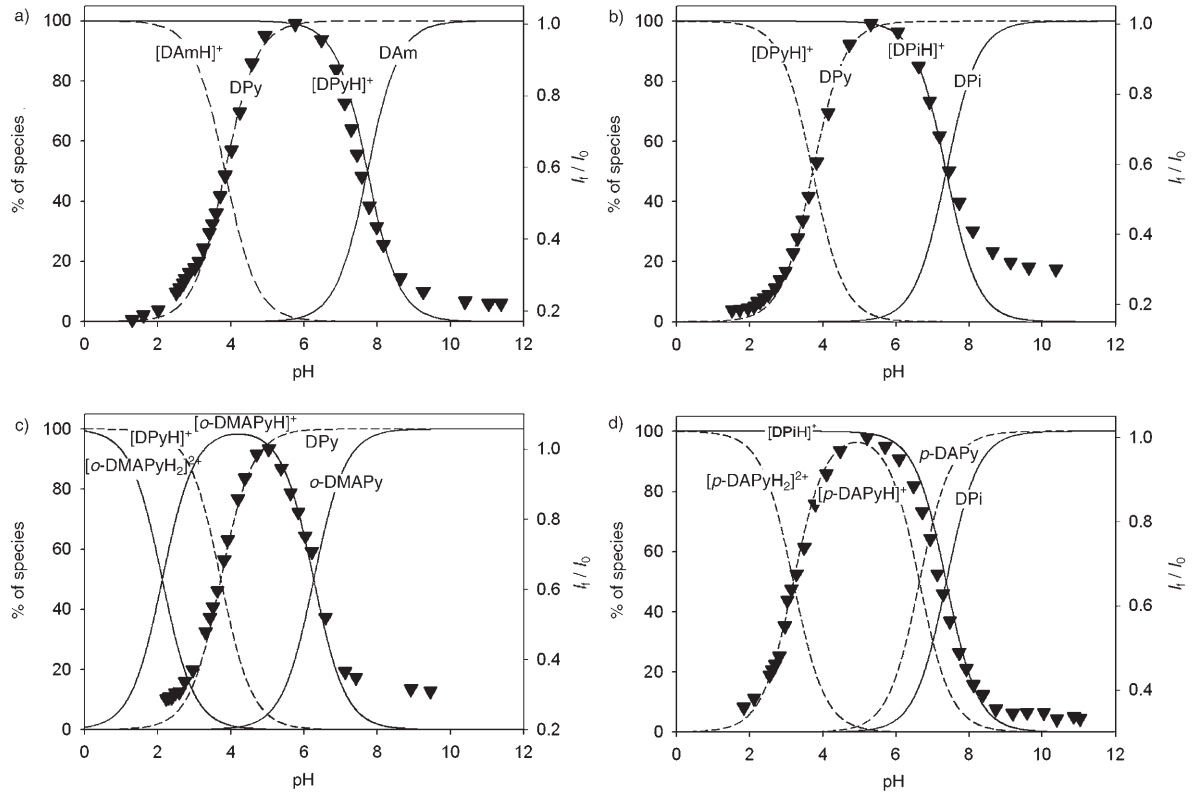

Figure 4. Black triangles represent the relative emission intensity (I_f/I_0) at 392 nm with varying pH (the maximum found emission in each series of spectra is considered as I_0). Solid and dashed lines represent % (with respect to total base) of each species present at the equilibrium with varying pH. The possible forms of each molecule (free, protonated and, where possible, diprotonated) are described by the same type of line (i.e., either solid or dashed). The species pertaining to each profile are indicated on the plots.

pH window with different limits (see Figure 3). Figure 4c reports the corresponding I_f versus pH profile that shows that the I_f is switched "off" in correspondence to the formation of [**DPy**H]$^+$ and of free ***o*-DMAPy**, while it is "on" only in the pH range in which free **DPy** and [***o*-DMAPy**H]$^+$ (protonation is on the amino group) coexist.

On the other hand, it should be emphasized that not all the combinations are allowed if an efficient signalling system is needed. The transition from the "off" to the "on" state, or viceversa, is superimposable to the distribution diagrams of the involved bases. Combinations of bases where the pyridine/amine pK_a values are similar (e.g. **DPy**/**DDAPy**) would result in an almost "always off" profile: at the same pH at which the pyridine group of one species is being deprotonated, the amine of the other species starts to be deprotonated as well. A significant quantity of a quenching group is therefore always present inside the micelles, allowing for only partial or even negligible fluorescence revival.

Finally, in order to further extend the flexibility of this approach, the secondary amine precursors of the R_2N-CH_2-Py molecules can be advantageously used. Preparation of ***o*-DMAPy**, ***p*-DMAPy**, **DDAPy** and **DMAMPy** (as described in the Experimental Section) passes through the tertiarization of the corresponding secondary amines, ***o*-DAPy** and ***p*-DAPy**, that can be schematically indicated as RNH-CH_2-Py.

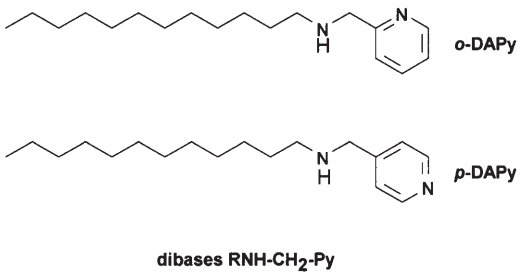

Secondary amines are less efficient quenchers than tertiary ones for polyaromatic hydrocarbon fluorophores, due to their intrinsically reduced electron donating properties [see for example, ref. [21]]. We studied the acid/base properties and the I_f versus pH behaviour in micelles of (*N*-dodecyl)-2-aminomethylpyridine (***o*-DAPy**) and (*N*-dodecyl)-4-aminomethylpyridine (***p*-DAPy**) under the usual experimental conditions. For ***o*-DAPy** we found $\log K_1 = 5.08$ (± 0.01) and $\log K_2 = 2.62$(± 0.02), while for ***p*-DAPy** $\log K_1 = 6.65$(± 0.02) and $\log K_2 = 3.20$ (± 0.02). The I_f versus pH profile, determined by means of pH–fluorimetric titrations of these micellized molecules (10^{-3} M), does not feature a fluorescent window but it is just of the "on–off" type. Superposition with the relative distribution diagram (see Supporting Information) shows that only the protonated pyridine moiety is

an efficient quencher, while the free secondary amine moiety does not quench pyrene fluorescence (lowering in intensity of less than 5% is observed for RNH-CH_2-Py with respect to $[RNH_2\text{-}CH_2\text{-}Py]^+$ for both systems). Accordingly, ***o*-DAPy** and ***p*-DAPy** are dibasic molecules with just one pH-sensitive quenching fragment. In order to obtain a system signalling a pH window with different limiting values, we choose to combine ***p*-DAPy** and **DPi**, which are dictated by ***p*-DAPy** logK_2 (3.20) and by **DPi** log$K$ (7.38). The corresponding I_f versus pH profile, obtained from a 5×10^{-4} M solution of both bases in the usual pyrene/Triton X-100 medium, is displayed in Figure 3d, which also shows a satisfactory superposition of the profile to the expected curves of the distribution diagram.

Experimental Section

Synthesis and materials: Pyrene (97%, Fluka) was used as received. Triton X-100, that is, *tert*-octylphenoxy polyoxyethylene glycol with and average of 9–10 oxyethylene units, was purchased from Caledon (average molecular weight = 647). *N*,*N*′-Dimethyl-*N*″-dodecylamine (**DAm**) was purchased from Aldrich and used as received. 2-Dodecyl-pyridine (**DPy**) was prepared according to a described procedure.[22] The secondary amines (*N*-dodecyl)-2-aminomethylpyridine (***o*-DAPy**), (*N*-dodecyl)-4-aminomethylpyridine (***p*-DAPy**) and (*N*-dodecyl)-2-methyl-6-aminomethylpyridine (**DAPyM**) were prepared by formation of the Schiff bases (i.e., by mixing commercially available 2-pyridinealdehyde, 4-pyridinealdehyde or 6-methyl-2-pyridinecarboxaldehyde with dodecylamine in methanol), followed by reduction with excess $NaBH_4$ and hydrolysis, according to a well established procedure. The obtained products were characterized by IR and ESI mass spectroscopy and used for the preparation of the tertiary amine derivatives (***o*-DAPy** is already described in literature; see reference [23]).

***N*-dodecylpiperidine (DPi)**: Dodecylbromide (1.0 g, 4.01 mmol) and piperidine (0.342 g, 4.02 mmol) were dissolved in CH_3CN (50 mL) in a 100 mL flask containing K_2CO_3 (0.4 g). The mixture was refluxed overnight and, after cooling at room temperature, the solvent was evaporated under reduced pressure. The product was treated with water (50 mL) and the obtained solution was extracted with CH_2Cl_2 (3×50 mL). The combined organic extracts were dried over Na_2SO_4, filtered and evaporated (0.93 g, 92%). ^{1}H NMR ($CDCl_3$): δ = 2.32 (t, 2H; N-CH_2-$(CH_2)_n$-CH_3), 2.25 (t, 4H; N-CH_2- piperidine ring), 1.6–1.2 (m, 26H; CH_2 dodecyl chain and piperidine ring), 0.88 (t, 3H; -$(CH_2)_n$-CH_3); ESI MS: m/z: calcd for $C_{17}H_{35}N$; found: 254 [**DPi**+H^+].

(*N*-Methyl,*N*′-dodecyl)-2-aminomethylpyridine (*o*-DMAPy): (*N*-dodecyl)-2-methylaminopyridine (***o*-DAPy**, 276.5 mg, 1.0 mmol) was dissolved in formic acid (1.1 mL, 27.4 mmol) and formaldehyde (1.1 mL, 11 mmol). After 16 h of reflux and stirring the reacted mixture was cooled at room temperature and treated with 20 drops of 37% HCl. Evaporation under reduced pressure yielded a solid which was dissolved in NaOH (2 M, 28 mL). The obtained solution was extracted with chloroform (3×50 mL). The combined organic extracts were dried over Na_2SO_4, filtered and evaporated to give DMP as a white wax (250 mg, 86%). ^{1}H NMR ($CDCl_3$): δ = 8.65 (d, 1H; pyr), 7.60 (t, 1H; pyr), 7.41 (d, 1H; pyr), 7.15 (t, 1H; pyr), 3.67 (s, 2H; py-CH_2-N), 2.40 (t, 2H; N-CH_2-$(CH_2)_n$-CH_3), 2.25 (s, 3H; N-CH_3), 1.6–1.2 (m, 20H; CH_2 dodecyl chain), 0.88 (t, 3H; -$(CH_2)_n$-CH_3); ESI MS: m/z: calcd for $C_{19}H_{34}N_2$; found: 291 [***o*-DMAPy**+H^+].

(*N*-Methyl,*N*′-dodecyl)-4-aminomethylpyridine (*p*-DMAPy): (*N*-dodecyl)-4-aminomethylpyridine (***p*-DAPy**, 1.0 g, 3.62 mmol) was dissolved in formic acid (3.97 mL, 99.2 mmol) and formaldehyde (3.99 mL, 39.8 mmol). After 16 h under reflux and stirring, the reacting mixture was cooled at room temperature and treated with 23 drops of concentrated HCl (37%). The acid was evaporated under reduced pressure. The residue was dissolved in NaOH (2 M, 27.6 mL) and the obtained solution was extracted with chloroform (3×50 mL). The combined organic extracts were dried over Na_2SO_4, filtered and evaporated (0.81 g, 77%). ^{1}H NMR ($CDCl_3$): δ = 8.62, 7.43 (2d, 2×2H; pyr), 3.64 (s, 2H; py-CH_2-N), 2.36 (t, 2H; N-CH_2-$(CH_2)_n$-CH_3), 2.26 (s, 3H; N-CH_3), 1.5–1.2 (m, 20H; CH_2 dodecyl chain), 0.90 (t, 3H; -$(CH_2)_n$-CH_3); ESI MS: m/z: calcd for $C_{19}H_{34}N_2$; found: 291 [***p*-DMAPy**+H^+].

(*N*-Methyl,*N*′-dodecyl)-2-methyl-6-aminomethylpyridine (DMAMPy): **DAPyM** (290.5 mg, 1.0 mmol) was treated with the same procedure described for **p-DMAPy**. Yield: 247 mg, 81%. ^{1}H NMR ($CDCl_3$): δ = 7.81 (t, 1H; pyr), 7.43 (d, 1H; pyr), 7.20 (d, 1H; pyr), 3.80 (s, 2H; py-CH_2-N), 2.60 (s, 3H; CH_3-py), 2.37 (t, 2H; N-CH_2-$(CH_2)_n$-CH_3), 2.25 (s, 3H; N-CH_3), 1.5–1.2 (m, 20H; CH_2 dodecyl chain), 0.91 (t, 3H; -$(CH_2)_n$-CH_3); ESI MS: m/z: calcd for $C_{20}H_{36}N_2$; found 305 [**DMAMPy**+H^+].

(*N*,*N*′-Didodecyl)-2-aminomethylpyridine (DDAPy): ***o*-DAPy** (1.0 g, 3.62 mmol) was dissolved in CH_3CN (70 mL) in a 100 mL flask containing K_2CO_3 (400 mg, 2.86 mmol). Dodecylbromide (812 μL, 3.62 mmol) was added under stirring and the solution was refluxed for 24 h. The reaction was stopped when the reagents were completely consumed (controlled by TLC: alumina; hexane/acetate 4:1). The carbonate was filtered off and the solvent was evaporated under reduced pressure to obtain a pale yellow oil (1.22 g, 76%). ^{1}H NMR ($CDCl_3$): δ = 8.66 (d, 1H), 7.59 (t, 1H; pyr), 7.42 (d, 1H; pyr), 7.20 (t, 1H; pyr), 3.70 (s, 2H; py-CH_2-N), 2.38 (t, 4H; N-CH_2-$(CH_2)_n$-CH_3), 1.5–1.2 (m, 40H; CH_2 dodecyl chains), 0.90 (t, 6H; -$(CH_2)_n$-CH_3); ESI MS: m/z: calcd for: $C_{30}H_{56}N_2$; found 445 [**DDAPy**+H^+].

Titrations: Protonation equilibria of monodispersed species were studied in 0.05 M tetrabutylammonium nitrate water/dioxane mixtures (2:8 v/v), at 25 °C, by titrating a solution containing the chosen molecule and excess nitric acid with standard base (KOH). Electrode calibration and potentiometric measurements were carried out as already described.[24] Protonation equilibria of micellized species were studied in water containing 6.47 g L^{-1} of Triton X100, by addition of standard base (KOH) to a 10^{-3} M solution of the chosen molecule containing excess standard nitric acid. Solutions were prepared to contain 0.05 M $NaNO_3$ as the supporting electrolyte, T = 25 °C. Potentiometric measurements were carried out automatically, as already described.[24] The titration curves were fitted and the equilibrium constants were calculated by using the nonlinear fitting program HYPERQUAD.[16]

Coupled pH–spectrofluorimetric titrations were carried out on water solutions containing 6.47 g L^{-1} of Triton X-100, 9×10^{-6} M pyrene (dissolved by adding aliquots of concentrated pyrene solutions in t-butanol, final t-butanol concentration < 0.5% v/v), 10^{-3} M of the chosen mono- or dibase (or 5×10^{-4} M each when two different molecules were combined) and 0.05 M $NaNO_3$, at 25 °C. Bulk solutions of 50–70 mL were used (kept under a constant flow of nitrogen), treated with excess nitric acid and titrated by manual micropipette additions of 10–50 μL aliquots of standard KOH. A glass electrode for pH measurement was dipped in the bulk solution. At each base addition the pH was recorded and a portion of 2–3 mL of the bulk solution was transferred into a cuvette. The emission spectra were recorded in the spectrofluorimeter (λ_{exc} = 340 nm) and the portion of solution was transferred to the bulk, prior to the next KOH addition. Total KOH addition, at the end of the titrations, did not exceed 0.3 mL. Further pH–spectra measurements were added in some cases at the end of the titration to better explore the more acidic zone (pH 0–2) by addition of 10 M HNO_3 in 10–50 μL aliquots.

Instrumentation: Mass spectra were recorded on a Finnigan MAT TSQ 700 instrument; NMR spectra on a Bruker AMX 400. Spectrofluorimetric measurements were performed with a Perkin Elmer LS 50B instrument. The pH titrations were made with a Radiometer TitraLab 90 titration system.

Acknowledgements

Thanks are due to Università di Pavia (CICOPS granting 2004, FAR 2005) and to MIUR (Ministero dell'Istruzione, dell'Università e della Ricerca, project FIRB RBNE019H9K-002) for financial support.

[1] M. Wolszczak, J. Miller, *J. Photochem. Photobiol. A* **2002**, *147*, 45.
[2] R. G. Alargova, I. I. Kochijashky, M. L. Sierra, R. Zana, *Langmuir* **1998**, *14*, 5412.
[3] a) P. P. Infelta, M. Gratzel, J.K. Thomas, *J. Phys. Chem.* **1974**, *78*, 190; b) M. Tachiya, *Chem. Phys. Lett.* **1987**, *133*, 289.
[4] R. A. Bissel, A. J. Bryan, A. P. de Silva, C. P. McCoy, *J. Chem. Soc. Chem. Commun.* **1994**, 405.
[5] Y. Diaz-Fernandez, A. Perez-Gramatges, S. Rodriguez-Calvo, C. Mangano, P. Pallavicini, *Chem. Phys. Lett.* **2004**, *383*, 245.
[6] a) A. W. Czarnik, *Acc. Chem. Res.* **1994**, *27*, 302; b) A. P. De Silva, D. B. Fox, A. J. M. Huxley, T. S. Moody, *Coord. Chem. Rev.* **2000**, *205*, 41; c) R. Martinez-Manez, F. Sancenon, *Chem. Rev.* **2003**, *103*, 4419; d) B. Valeur, I. Leray, *Coord. Chem. Rev.* **2000**, *205*, 3.
[7] M. Huston, K. Haider and A. W. Czarnik, *J. Am. Chem. Soc.* **1988**, *110*, 4460.
[8] P. Grandini, F. Mancin, P. Tecilla, P. Scrimin, U. Tonellato, *Angew. Chem.* **1999**, *111*, 3247; *Angew. Chem. Int. Ed.* **1999**, *38*, 3061.
[9] M. Berton, F. Mancin, G. Stocchero, P. Tecilla, U. Tonellato, *Langmuir* **2001**, *17*, 7521.
[10] K. Niikura, E. V. Anslyn, *J. Org. Chem.* **2003**, *68*, 10156.
[11] Y. Diaz Fernandez, A. Perez Gramatges, V. Amendola, F. Foti, C. Mangano, P. Pallavicini, S. Patroni, *Chem. Commun.* **2004**, 1650.
[12] a) L. Fabbrizzi, F. Gatti, P. Pallavicini, L. Parodi, *New J. Chem.* **1998**, *22*, 1403; b) P. Pallavicini, V. Amendola, C. Massera, E. Mundum, A. Taglietti, *Chem. Commun.* **2002**, 2452; c) V. Amendola, C. Mangano, P. Pallavicini, *Dalton Trans.* **2004**, 2850.
[13] T. Gunnlaugsson, *Tetrahedron Lett.* **2001**, *42*, 8901.
[14] a) A. P. de Silva, H. Q. N. Gunaratne, C. P. McCoy, *Chem. Commun.* **1996**, 2399; b) S. A. de Silva, A. Zavaleta, D. E. Baron, O. Allam, E. V. Isidor, N. Kashimura, J. M. Precarpio, *Tetrahedron Lett.* **1997**, *38*, 2237; c) S. A. de Silva, B. Amorelli, D. C. Isidor, K. C. Loo, K. E. Crooker, Y. E. Pena, *Chem. Commun.* **2002**, 1360.
[15] a) R. J. Jobson, E. A. Dennis, *J. Phys. Chem.* **1977**, *81*, 1075; b) M. Wolszczak, J. Miller, *J. Photochem. Photobiol. A* **2002**, *147*, 45.
[16] P. Gans, A. Sabatini, A. Vacca, *Talanta* **1996**, *43*, 1739.
[17] V. Frenna, N. Vivona, G. Consiglio, D. Spinelli, *J. Chem. Soc. Perkin Trans. 2* **1985**, 1865.
[18] K. Kahmann, H. Sigel, H. Erlenmeyer, *Helv. Chim. Acta* **1964**, *47*, 1754.
[19] L. Alderighi, P. Gans, A. Ienco, D. Peters, A. Sabatini, A. Vacca, *Coord. Chem. Rev.* **1999**, *184*, 311.
[20] The range of 0–12 is the suggested operating range of the glass electrode we utilized for pH measurements (radiometer pHG201–7). A slight and reversible decrease in the I_f intensity (less than 10%) is observed in very acidic solutions (pH 0–1.5). The same effect is observed even in the absence of water-soluble bases (i.e., with TritonX-100 and pyrene only), and may be attributed to changes in the polarity of the micellar microenviroment that can cause a decrease of pyrene fluorescence lifetime.
[21] V. Amendola, L. Fabbrizzi, C. Mangano, P. Pallavicini, A. Perotti, A. Taglietti, *J. Chem. Soc. Dalton Trans.* **2000**, 185.
[22] F. Brody, M. P. Bogert, *J. Am. Chem. Soc.* **1943**, *65*, 1075.
[23] P. Scrimin, P. Tecilla, U. Tonellato, *J. Org. Chem.* **1991**, *56*, 161.
[24] V. Amendola, L. Fabbrizzi, P. Pallavicini, L. Parodi, A. Perotti, *J. Chem. Soc. Dalton Trans.* **1998**, 2053.

Received: May 31, 2005
Published online: September 30, 2005

